Abundance and Genetic Significance of Lithium in Karst-Type Bauxite Deposits: A Comparative Review

Maria Economou-Eliopoulos *[ID] and Christos Kanellopoulos [ID]

Department of Geology and Geoenvironment, National and Kapodistrian University of Athens,
15784 Athens, Greece; ckanellopoulos@gmail.com
* Correspondence: econom@geol.uoa.gr

Abstract: Palaeo weathering during the Cretaceous–Eocene interval is most favorable for bauxitization, i.e., transport and deposition in traps on the karstified surfaces of the Mediterranean karst bauxite belt, including the Parnassos–Ghiona bauxite deposit. Resources of lithium (Li), a critical metal of strategic significance in karst-type bauxite deposits, have attracted significant attention in recent years. Due to the discovery of the Li enrichment in certain karstic bauxite deposits in Europe and particularly in China, this review study is focused on the unexplored Li content in the Parnassos–Ghiona (Greece) bauxite deposit, aiming to improve the understanding of the major controlling factors for their origin and enrichment of critical metals. The presence of thin (up to 50 cm) pyrite-bearing coal seams and carbonaceous facies on top of the Parnassos–Ghiona bauxite deposit, at the transition between B3 (the youngest) bauxite horizon and the occurrence of multicolor bauxite ores reflecting a multistage evolution and changes in the mineralogy and geochemistry, is a common feature with other bauxite deposits in Europe and elsewhere. The organic matter, such as microorganisms in coal layers and carbonaceous layers (derived from plants and algae growing in paleo-mires after a regression of the sea), contains Li, which is derived from seawater, as suggested by a positive correlation with B (a seawater component as well). The available geological, mineralogical, and geochemical data highlight the particular significance of coal layers and carbonaceous layers overlying bauxite bodies as a driving force for redox reactions and as a source of Li in the exploration of karst-type bauxite deposits.

Keywords: bauxite; karst-type; critical; lithium (Li); bio-mineralization; metal cycling

1. Introduction

The karst-type bauxites, characterized by a karstic carbonate bedrock, account for approximately 11.5% of the global bauxite resources, while 88% belong to the lateritic-bauxite deposits [1]. Greece is the eight largest bauxite producer worldwide and the largest in the E.U. [2]. Bauxite deposits of karst type are well known in the Parnassos–Ghiona mountains [3–7] and Montenegro (Adriatic zone coastal area), belonging to the Dinaric metallogenetic province [1,8]. Commonly, the bauxites are red-colored and contain diaspore, boehmite, goethite, and hematite. Recently, many studies have focused on transitional zones from typical red bauxite to grey, pinkish-white, and very pale yellow varieties characterized by multistage changes in the Fe-mineral assemblage, pyrite, and Fe-oxides, high aluminum content (up to 80 wt.% Al_2O_3), and the role of changes in the mineralogical composition of bauxite deposits in Greece, Hungary, Croatia, Turkey (Doğankuzu and Mortaş, Taurides), and elsewhere [5,7,9–14].

The global demand for critical and strategic minerals is expected to significantly increase as the world increasingly transitions to clean energy and other clean technologies. The list of critical and strategic metallic elements for the U.S.A. and the European Union includes rare earth elements (REE), aluminum (Al), lithium (Li), gallium (Ga), vanadium (V), platinum-group elements (PGE), antimony (Sb), beryllium (Be), bismuth (Bi), cesium

(Cs), chromium (Cr), cobalt (Co), germanium (Ge), hafnium (Hf), indium (In), magnesium (Mg), manganese (Mn), nickel (Ni), niobium (Nb), rubidium (Rb), strontium (Sr), tantalum (Ta), tellurium (Te), tin (Sn), titanium (Ti), tungsten (W), zinc (Zn), and zirconium (Zr). It is well-known that karst-type bauxites can be considered as potential mineral raw materials for obtaining rare earth elements (REEs). Thus, in addition to aluminum, the main metals in bauxite deposits are an important source of REEs, including Ga, Sc, and V [8,12,14–20]. Lithium demand has increased due to its increasing use in batteries. More than 73% of lithium resources are distributed in North and South America, and relatively few (7%) are distributed in Europe (data from S&P global market intelligence, 2021) [21]. Although the primary economic sources for Li are brines, salt lakes, and pegmatite deposits [22], Li resources in karst bauxite have attracted much attention in recent years due to the discovery of Li super-enrichment in certain karstic bauxite deposits, such as the Permian Li-rich karstic bauxites in central Yunnan province, western margin of the South China Block [18–20]. To our knowledge, the Li content in the bauxite ores of Greece remains unexplored, although the Li content is included among trace elements in the Parnassos–Ghiona deposit [7,14]. The present review study is focused on critical metals in karst-type bauxites from Greece, such as Li, Ga, V, Sc, rare earth elements (REE), and platinum-group elements (PGE), with emphasis on Li, in an attempt to improve the understanding of major controlling factors for their origin and enrichment.

2. Materials and Methods

Although the analytical methods applied for determining major and trace elements in bauxite ore are provided in various publications [5–8,12,15,17,19], a brief outline is given here. Due to the heterogeneous character of most bauxite deposits, samples of a minimum weight of 2 kg were collected from surface exposures and underground bauxite mines. Minor and trace elements were obtained using inductively coupled plasma mass spectrometry (ICP–MS) analysis after multi-acid digestion (HNO_3–$HClO_4$–HF–HCl) at the ACME Laboratories Ltd., Vancouver, BC, Canada. Platinum-group element (PGE) analyses were carried out using the Ni-sulfide fire-assay pre-concentration technique, with the nickel fire-assay technique from large (30 g) samples at Genalysis Laboratory Services, Perth, Australia. This method allows for the complete dissolution of samples. The detection limits were 1 ppb for Pd, 10 ppb for Pt, and 5 ppb Au. The CDN–PGMS–23 was used as a standard. Thin polished sections of bauxites were investigated using a reflected light microscope, a scanning electron microscope (SEM), and energy dispersive spectroscopy (EDS). The SEM–EDS semi-quantitative analyses were carried out at the Department of Geology and Geoenvironment, National and Kapodistrian University of Athens (NKUA), using a JEOL JSM 5600 SEM (JEOL, Tokyo, Japan) equipped with the ISIS 300 OXFORD automated energy dispersive X-ray analysis system. The analytical conditions included a 20 kV accelerating voltage and a 0.5 nA beam current.

3. Geological Outline

The Cretaceous–Eocene interval is considered the most favorable for bauxitization. Therefore, bauxitic material has been transported and deposited in traps on karstified surfaces [1,3]. Part of the Mediterranean karst bauxite belt are the Parnassos–Ghiona bauxite deposits of Greece. Three bauxite formations, B1, B2, and B3 (first, second, and third bauxite horizons, respectively), from the oldest to the youngest, are hosted within carbonate rocks, have different ages (Figure 1), and are intercalated with shallow water limestone within a Late Jurassic to a Cretaceous sequence of the Parnassos–Ghiona zone (Figure 1) [4]. Minor bauxite occurrences hosted by the Upper Eocene limestone have been described in the areas of Nafpaktos, Smerna, and Pylos of Western Greece [23,24]. A salient feature is the presence of thin (up to 50 cm) pyrite-bearing coal seams and carbonaceous facies on top of the Ghiona (Pera-Lakkos) bauxite deposit, marking the roof transition between B3 bauxite and the hanging wall limestone [7]. Similarly, the karstic bauxites in Montenegro occur in three stratigraphic levels in the Middle Triassic, Jurassic, and Paleogene, while carbonaceous

facies and grey–white karst bauxites are of the Cretaceous age [8,25–27]. Similar pyrite assemblages were documented in the Doğankuzu and Mortaş Upper Cretaceous bauxite deposits in the Seydişehir region in Turkey [11]. Salient features include the occurrence of thin coal layers overlying the bauxite deposits, and overthrusting, faulting, and the disruption of the continuity of the bauxite bodies are common characteristics [4,7]. The intense tectonism facilitating the meteoric fluid circulation in these bauxite deposits has produced a significant proportion (approximately 30% volume) of transformed red bauxite ore to whitish–grey, while yellow bauxite gradually grades downwards [5,6,28], as shown in Figure 1. The widespread occurrence of grey–white karst bauxites of the Cretaceous age is also a common characteristic in the Montenegro bauxite deposit [8,25,27,29].
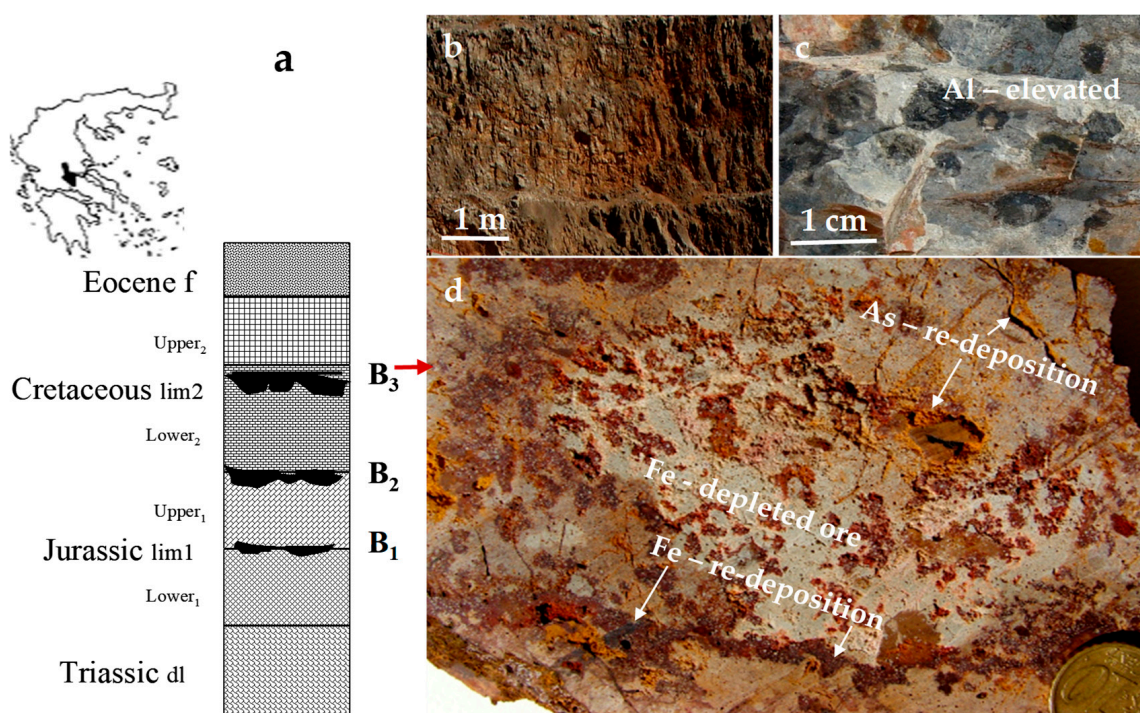

Figure 1. Location map and stratigraphic column of the Parnasso–Ghiona bauxite deposits. Symbols: dl = dolomitic limestone; lim1 = grey (lower) and dark colored (upper) Jurassic limestone; lim2 = limestone; f = flysch, overlain by quaternary conglomerates; B1 = Ffrst bauxite horizon, B2 = second bauxite horizon, B3 = third bauxite horizon (**a**). Photos of bleached and re-deposited parts of bauxite ore body showing the relationship between red, yellow, white, and re-precipitated zones along fractures (**b**–**d**).

4. Characteristic Features of Bauxite Deposits

4.1. Mineralogy and Texture

The main components of bauxite are boehmite and diaspore, forming pisoliths and oolites (Figure 2A,B), which are common. Gibbsite ilmenite, rutile, chromite, zircon, lithioporite, baddeleyite, chamosite, and quartz are present in lesser amounts (Figure 2) [4,6,7,12,15,30,31]. REE occurs mainly in authigenic/diagenetic REE–carbonate and phosphate minerals [15]. The presence of Th in diaspores and Fe-Cr-Ti-bearing diaspores have been described by Gamaletsos (2014) [30]. In a recent investigation [14], the mineralogical and geochemical composition of four vertical profiles from underground workings was recorded for the main oxy-hydroxides at the Agia Anna mine, including diaspore, goethite, anatase, and rutile as the main minerals. These minerals were characterized by deep red color. At the Variani and Shila mines, boehmite is abundant, kaolinite is widespread, and pyrite is rare. A salient feature in the Agia Anna bauxite profile is an increase in diaspore amount toward the top of the profile and the increasing amount of kaolinite toward the bottom [14].
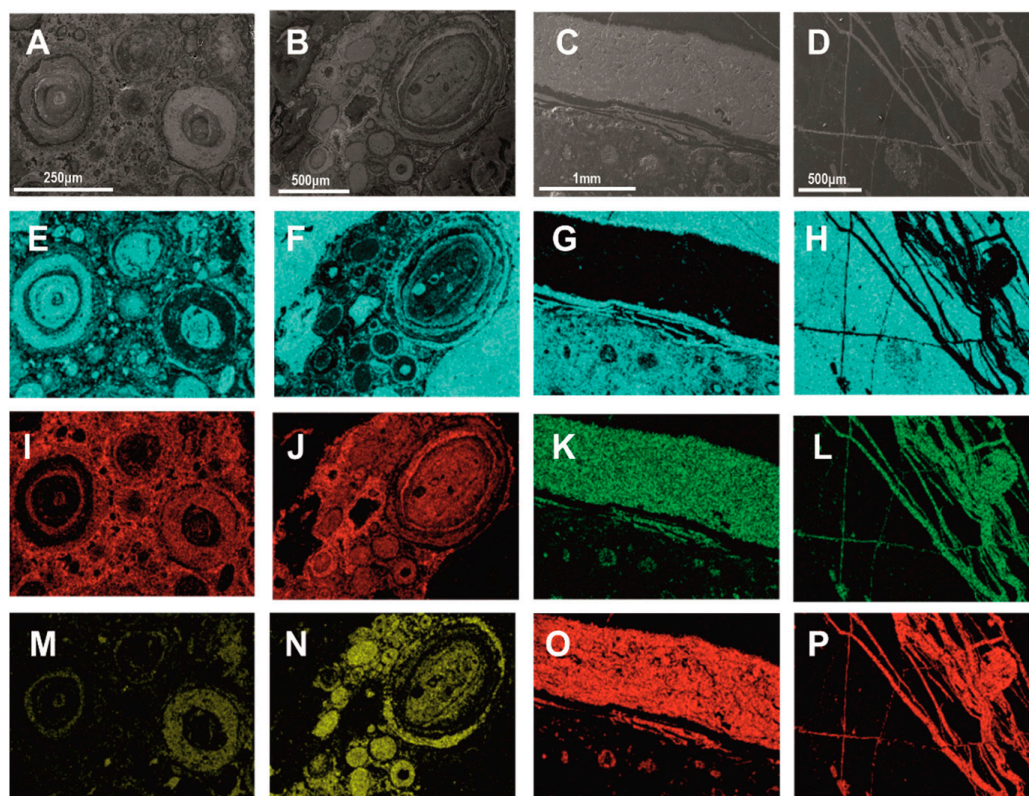
Figure 2. Back-scattered electron images (BSEI) of bauxite ores from the Parnassos–Ghiona deposit. (**A,B**): pisoliths and oolites, (**C,D**): sulfide-rich zone, (**E–P**): false color BSEI results of the mapping, displaying the distribution of Al: (**E–H**), Fe: (**I–L**), Si: (**M,N**), and S: (**O,P**).

The texture characteristics of multicolor bauxite ores (Figure 1b–d) are associated with thrust-fault affected parts of the Parnassos–Ghiona bauxite ores, reflecting a multistage evolution of the mineralogy and mineral chemistry. Sulfide-rich zones and thin sulfide layers (Figure 2) underlying transformed bauxite bodies and fossilized microorganisms of different morphological forms (filament, cocci-type) and sizes in close association with framboidal pyrite and Fe-oxides have been described in multicolor bauxite ores [5,6].

4.2. Geochemistry

4.2.1. Critical Metals in Bauxite Ores

Bauxite samples from the Parnassos–Ghiona deposit and small bauxite occurrences (Nafpaktos, Smerna, Pilos, Glyfa, Atalanti, Greece) have been analyzed for all PGE and Au, showing average values of 4.1 ppb Pd, 2.3 ppb Pt, 1.5 ppb Rh, and 24 ppb Au [14,28,32], which are lower than those in bauxite laterites and Ni-laterites [28]. The Pd/Pt ratio (2.12) is approximately the same in multicolor ores, with a mean of 0.8 ppb Pt, 1.7 ppb Pd, and 44 ppb Au, and in red–brown bauxite (Pd/Pt ratio 2.33), with a mean of 0.3 ppb Pt, 0.7 ppb Pd, and 31 ppb Au. The best-pronounced inter-element relationships have a positive correlation between Pd and As and a negative correlation with Sc and Ce [28].

Geochemical data on the Parnassos–Ghiona bauxite ores from previous studies have shown a range of 39 to 80 wt.% Al_2O_3 and wide variations of major and trace elements, including rare earth elements (REE), platinum-group elements (PGE), Ga, Sc, and V along bauxite profiles [5–7,14,15,28,32,33]. Representative analyses of bauxite ores from the Parnassos–Ghiona deposit are given (Table 1), while plots of critical metals versus Al_2O_3 content or samples from various deposits (Figure 3) show a wide variation, except those from Italy [7,8,14,19,27,30–40].

Table 1. Representative analyses (major and trace elements) of karst-type bauxite ores from the Parnassos–Ghiona deposit. Sources: [7,14,15,30].

	Bauxite Ores									Carbonaceous Shale	
Horizon	B2	B2	B3	B3	B3	B3	B3	B3	B3	B3	B3
Location	Proussorema		Frousia		Pera Lakkos		Agia Anna		Variani	Pera Lakkos	
wt.%	PR-12	PR-5	Ff17	F20	PL-grey	PL-red-brown	PS1-1	PS-1-4	PSS2-5	1-3cs	2-11cs
SiO_2	9.6	15.0	32.1	2.24	0.08	0.75	4.4	1.7	5.1	19.64	24.65
Al_2O_3	39.11	60.1	41.4	60.64	79.2	61.7	53.54	54.5	49.96	14.1	22.7
Fe_2O_{3T}	21.2	4.1	10.58	21.2	1.7	21.95	23.0	25.9	24.52	3.7	0.9
MnO	0.43	0.27	n.d.	0.01	n.d.	0.01	n.d.	n.d.	0.01	n.a.	n.a.
MgO	1.25	0.43	0.28	0.03	0.11	n.d.	0.9	n.d.	0.87	0.66	0.56
K_2O	2.39	1.25	0.14	n.d.	n.d.	n.d.	n.d.	n.d.	0.02	1.96	3.01
TiO_2	0.13	2.37	1.8	2.35	3.35	2.63	4.3	3.1	3.5	0.63	1.1
CaO	0.06	0.13	0.22	0.92	n.d.	n.d.	n.d.	n.d.	0.19	14.3	6.36
Na_2O	0.11	0.06	0.19	0.06	n.d.	n.d.	0.01	0.01	0.02	0.24	0.18
P_2O_5	15.7	0.11	0.05	0.05	0.01	0.02	0.03	0.02	0.07	n.a.	n.a.
LOI	20.5	15.7	13.5	12.9	14.91	12.18	13.85	15.05	13.6	n.a.	n.a.
Total	99.1	99.5	100.26	100.4	99.36	99.24	100.0	100.28	97.86		
ppm											
Li	n.a.	n.a.	n.a.	n.a.	n.a.	n.a.	60	30	90	226	367
Ga	n.a.	n.a.	n.a.	n.a.	84	66	75	66	65	22	46
Sc	n.a.	n.a.	n.a.	n.a.	30	51	28	28	25	n.a.	n.a.
V	n.a.	n.a.	n.a.	n.a.	520	620	330	380	480	350	240
La	390	220	42	58	6.1	83	69	41	9.6	16	69
Ce	98	830	67	36	106	99	260	26	217	38	228
Pr	870	6.3	203	125	1.8	12	14	11	2.3	4.2	17
Nd	27	70	19	7.2	6.3	35	47	44	8.5	15	69
Sm	230	250	68	28	2.3	7.8	8	9.2	2.1	2.7	14.5
Eu	75	49	15	7.7	0.4	1.9	1.7	2	0.54	0.5	3.3
Gd	17	7.8	2.9	1.8	1.03	9.1	7.7	8.3	3.32	2.8	16.6
Tb	1700	1430	420	260	0.7	2.8	1.5	1.6	0.8	0.4	2.2
Dy	83	39	12	8.6	4.7	18	12	10	5.5	2.2	13
Ho	12	5.3	1.7	1.5	1.05	3.9	2.6	2.3	1.24	0.5	2.6
Er	64	31	10	9.4	3.5	12.5	8.8	7.3	4	1.5	7.1
Tm	12	6.8	1.8	2.1	0.6	2	1.5	1.2	0.6	0.2	0.9
Yb	30	18	5.9	6.3	3.05	13	10.4	8.6	4.1	1.5	5.6
Lu	3.9	2.5	0.9	1	0.7	2.3	1.6	1.4	0.6	0.2	0.8
Y	21	15	7	8	31	71	70	57	34	11	72
Σ REE	3630	2980	880	560	170	370	576	230	384	323	890

n.a. = not available; n.d. = no detected.

Approximately 90% of Ga is derived from the recovery of bauxite [34]. The content of Ga in the Parnassos–Ghiona deposit shows a wide variation, ranging from 58 to 108 ppm (mean 67 ppm) of Ga (Table 1). It also exhibits a good positive correlation with Al_2O_3 (Figure 3a). Vanadium presents an average value of 460 ppm, with a wide variation of 270 to 720 ppm V throughout the deposit [14,30]. Another critical element is Sc, which is classified as a rare earth element by the International Union of Pure and Applied Chemistry [35]. It ranges from 29 to 73 ppm (mean 47 ppm Sc). Recently, a combination of various techniques has been applied for the study of nano-mineralogy and nano-geochemistry karst-type bauxite from the Parnassos–Ghiona deposits [12,17]. Thus, considering the relationships between critical elements REE, Sc, Ga, and V occurring in elevated contents in the Parnassos–Ghiona karstic-type bauxite deposit, they are comparable to those from other bauxite deposits of the same type in Europe and show similar trends (Table 2; Figures 4 and 5).

The REE content is relatively low, although values as high as 3600 ppm ΣREE have been recorded in the B2 horizon, showing a wide variation throughout the bauxite horizons [6,15,23,30,31]. The REE patterns for both Fe-elevated and Fe-depleted types are linked with a distinct positive Ce anomaly [30,31]. However, in transitional zones to coal and bauxite, both negative and positive values in the Ce/Ce* (Ce anomaly) have been recorded [30].
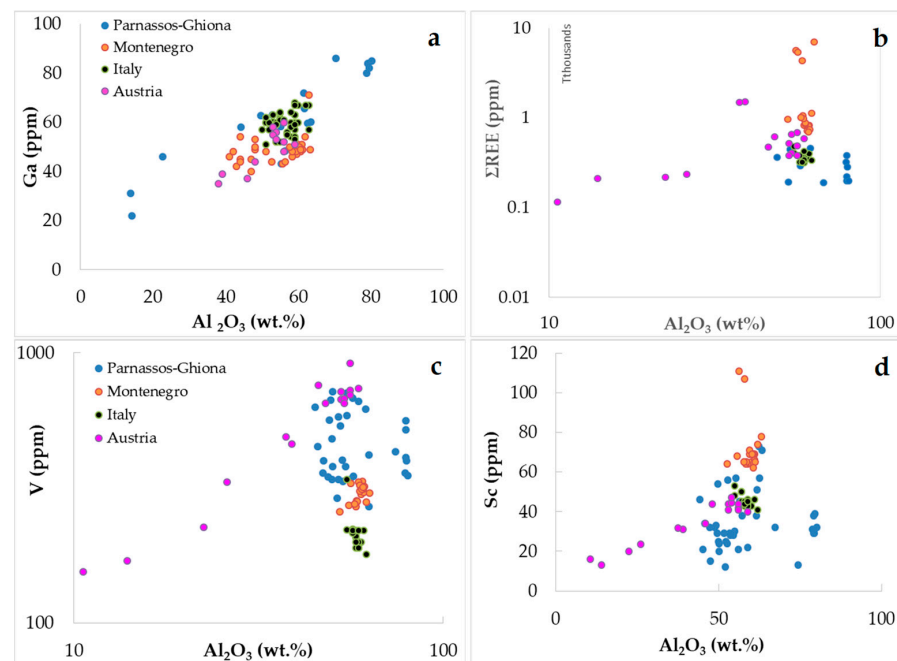
Figure 3. Plots of Ga, ΣREE, V, and Sc versus Al$_2$O$_3$ content (**a**–**d**) in selected bauxite deposits. Data sources: [7,8,14,19,27,30–40].
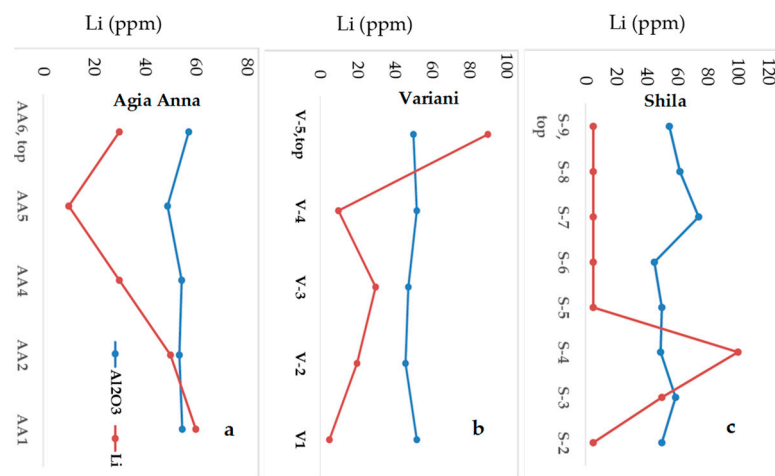

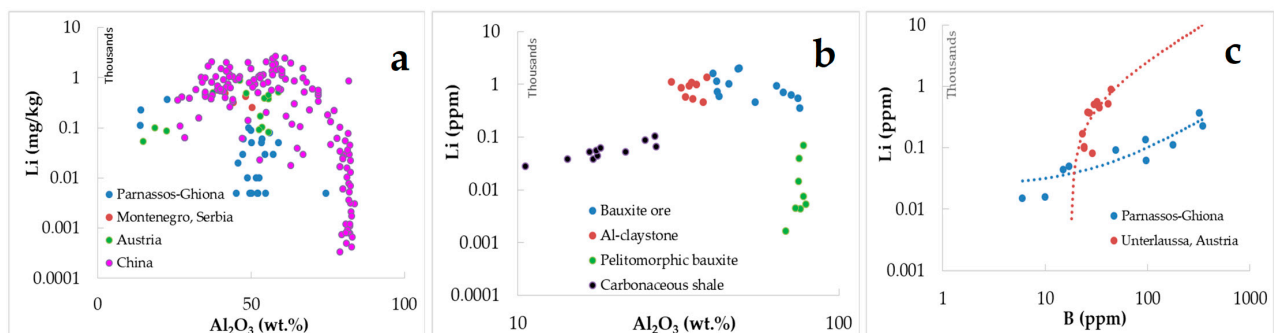**Figure 4.** Schematic compositional variations for Li and Al$_2$O$_3$ through vertical bauxite profiles based on the literature data (**a**–**c**) [14].

Figure 5. Plots of Al$_2$O$_3$ versus Li for individual bauxite deposits (**a**), various rock types from Central Yunnan, China (**b**), and Li versus B (**c**). Data from [14,19,39–41].

Table 2. Comparison of selected critical metal content between the Parnassos–Ghiona deposit and other bauxite deposits of Europe and China.

Location	Age (Ma)		Al_2O_3 (wt.%)	ΣREE (ppm)	Li (ppm)	Ga (ppm)	Sc (ppm)	V (ppm)	Thickness of Overlying Organic-Rich Sediments	Ref.
Greece										
Parnassos-Ghiona	Cretaceous	n = 22	45–74 (52.5)	123–444 (252)	5–90 (35)	58–108 (67)	12–38 (26)	330–720 (460)	Bauxite ore	[14]
Parnassos-Ghiona	Cretaceous	n = 3	14–22.7 (17)	83–345 (247)	111–526 (335)	22–46 (33)	n.a.	244–427 (343)	Carbonaceous shale	[7]
Parnassos-Ghiona	Cretaceous	n = 6	1.2–4.4 (2.2)	44–290 (87)	16–137 (67)	4.7–10 (7.8)	n.a.	21–121 (77)	Up to 50 cm coal seams	[7]
Serbia										
Montenegro	Cretaceous to Triassic	n = 16	41–62 (47.2)	310–1180 (770)	257–485 (370)	42–71 (49)	25–59 (44)	93–730 (346)	Bauxite ore	[8,27]
S. Italy	Cretaceous									
Otranto		n = 20	54–62 (58)	3150480 (340)	n.a.	52–68 (58)	41–54 (44)	190–249 (210)	Bauxite ore	[39]
Austria		n = 13	37.5–59 (51)	380–1550 (600)	99–900 (354)	35–60 (50)	31–44 (35)	464–920 (690)	Bauxite ore	[40]
Unterlaussa	Upper Cretaceous	n = 4	15–5-26 (20.5)	115–235 (220)	53–354 (150)	16–36 (25)	12–24 (18)	155–33 (220)	More than 1400 m mostly	[40]
Unterlaussa									organic-rich sediments	
China										
Yunnan	Upper Permian	n = 9	27–60 (48)	73–280 (156)	108–2060 (955)	30–115 (80)	21–50 (32)	110–206 (154)	Bauxite ore and Claystone	[20]
Guangxi	Upper Permian	n = 14	55–80 (74)	23–174 (64)	3–25.4 (10.4)	n.a.	n.a.	n.a.	Bauxite ore	[19]
Guangxi	Upper Permian	n = 11	37–54 (40)	26–116 (78)	1030–3388 (2590)	n.a.	n.a.	n.a.	Carbonaceous clays	[19]
									~10 m carbonaceous rocks and coal seams	

n.a. = not available; n.d. = no detected.

Recently, special attention has been given to new sources of lithium (Li), as it is a crucial strategic metal used in a number of modern industries, especially in battery storage and new energy technologies [19,20,22]. However, there are limited analytical data concerning the Li content in bauxites. The Li in the Parnassos–Ghiona deposit has been reported among other trace elements [7,14], but its content and significance have not been discussed. The available analytical data show that the Li content in the Parnassos–Ghiona deposit ranges from <10 to 90 ppm Li (mean 35), whereas the carbonaceous shales overlying the B3 bauxite horizon are characterized by significant Li content, ranging from 110 to 530 (mean 340) ppm Li [7] (Tables 1 and 2). Based on analytical data from the literature [7,14], the variation in the Al_2O_3 and Li content, along with the vertical profiles, are presented here. These data show that in the Agia Anna bauxite profile, the highest Li content appears at the bottom (Figure 4a), with the highest amount of kaolinite [14]. There is also a very good (Figure 5; r = 0.92) correlation between the Li and B contents in the coal and carbonaceous shales.

4.2.2. A Comparison between the Parnassos–Ghiona and Other Bauxite Deposits

Based on the type of bauxite deposit, its age, the range in the content of critical metals, and the existence of organic matter in overlying sediments the Parnassos–Ghiona bauxite deposit has been compared with selected other deposits. The occurrence of very high-grade bauxite ores of karst-type deposits have been described elsewhere within the Mediterranean Karst Bauxite belt, such as in the Croatian bauxites and the bauxites of Montenegro [36]. A salient feature that is highlighted in the present review study is the Li content in the Parnassos–Ghiona deposit, which is lower compared to that in Montenegro (Serbia) and other karst-type bauxite deposits of Europe and China (Table 2). Karst-type bauxite deposits in China account for approximately 95% of bauxite resources, located mainly in Northern and Southern China [18–20]. Recently, studies on karstic bauxite have focused on Li enrichment, in particular in claystone [19,20,37]. The upper Permian Guangxi bauxite deposit in the Pingguo area, China, is strongly enriched in Li. At the same time, the overlying clay rock layer (black carbonaceous clay rocks or coal seams) of approximately ~10 m thickness has shown significant enrichment in Li (up to 3388 ppm Li) [19], as shown in Table 2. Furthermore, the investigation of the bauxite deposit in northern Guizhou has shown that the Li in compact bauxite ores is mainly hosted in illite, whereas the Li in aluminous claystone is mainly hosted in kaolinite [19]. It was concluded that Li enrichment occurred at the primary bauxitic material formation stage in a coastal-restricted basin after transgression and water retention during hot and dry periods [37]. Italy is among the other European countries with karst-type bauxites. However, analytical data on the Li content in Italy are not available yet [38,39]. The B3 horizon of the Parnassos–Ghiona bauxite deposit is similar to the Cretaceous karst-type bauxite deposit of the Unterlaussa in Austria in terms of the presence of carbonaceous shale layers overlying the bauxite bodies and coal intercalations with sediments [7,40]. However, the bauxite deposit in Austria is overlain by a thick (>1400 m), diverse sediment succession consisting of coal, carbonaceous shale, sandstones with coal seams, intercaleceous of dark and light limestones, bituminous calcareous marls coarse conglomerates, dark bituminous marls and schists, and calcareous sandstone [40]. In addition, although the Li content in the Parnassos–Ghiona bauxite deposit is much lower than of the Unterlaussa deposit in Austria, both deposits exhibit a positive correlation with the B content (Figure 5).

4.2.3. The Greek Bauxite Metallurgical Residue (Red Mud)

The residue waste of the Bayer process or red mud during the alumina production in Greece [16,42] represents a potential secondary resource of critical metals. The REE content in Greek red mud seems to be remarkably increased to almost twice as much as that of the Parnassos–Ghiona bauxite ore [43,44]. The scandium in the red mud may be contained within detrital mineral phases, like Sc-bearing zircons [45], or may be adsorbed onto the surface of iron oxide phases [46]. Although the separation of Sc from the other elements is

not easy, due to the chemical similarities between Sc(III) and Fe(III), a methodology for full separation has been achieved [47]. Recently, a cost-effective methodology for the recovery of the Li has been proposed [20]. According to the authors, under the leaching conditions, phosphoric acid reacts with the Al and Li in the strong acid, producing salts, which are soluble in the solution.

5. Discussion

In general, unaltered parts of bauxite deposits and/or certain deposits of karst type are characterized by homogeneous compositions, such as the Apulian karst bauxite in Southern Italy and the Abruzzi (Central and Southern Apennine) karst bauxite deposit [38,39], as shown in Figure 3. Stronger compositional (major and trace elements) variations in karst-type bauxite deposits near the boundary of ore bodies with the host limestones is a common feature for many karst-type bauxite deposits (Table 2; Figures 3–5), which may be linked to deposition and/or post-deposition processes (diagenetic and epigenetic transformations). Specifically, there is an increasing trend of Ga, V, Li, As, Pd, and LREE with increasing Al_2O_3 content, particularly in highly fragmented parts, underlying faults, and in proximity to limestones (Figures 3–5; [42]). The occurrence of coal layers and carbonaceous layers overlying bauxite bodies [7,8,19,20,40] may be of particular significance as a source of certain bauxite components and as a driving force controlling redox conditions and, in turn, element cycling (mobility and re-precipitation) and mineral transformation.

5.1. Organic Matter as Driving Force of Redox Processes Reactions

The organic matter, such as coal and/or carbonaceous layers, overlying the Parnassos–Ghiona bauxite bodies, is considered to be derived from plants and algae growing in paleo-mires during a regression of the sea, on bauxite hosted in karstified limestone [7]. The petrological, mineralogical, and geochemical data point to the predominance of reducing conditions during the degradation of organic matter in the palaeomires [7]. The determination of carbon and oxygen isotopes in samples from the footwall limestones of the Greek bauxites have shown a $\delta^{13}C_{PDB}$ isotopic values of between −0.8 and −4.8‰ and $\delta^{18}O_{PDB}$ isotopic values of between −5.9 and +3.8‰ [6]. The more negative carbon isotopic values in the third horizon have been attributed to the increased deposition of organic matter and subsequent oxidation, resulting in fractionation of ^{12}C in CO_2 [6]. The presence of organic matter, such as coal and/or carbonaceous layers overlying bauxite bodies and/or a consortium of microorganisms at highly faulted zones throughout, may catalyze redox reactions [48–51]. Microorganisms of varying morphological forms have been described in the Parnassos–Ghiona bauxite deposits in detail [6,31]. The roles of microorganisms are to produce enzymes, catalyze redox reactions, and provide nucleation sites for the precipitation of secondary minerals such as bacteriomorphic goethite and pyrite. The negative $\delta^{34}S$ values for sulfide-bearing samples seems to be very important because they facilitate metal bioleaching and biomineralization under the appropriate conditions [6,7,31]. Under the activity of reducing microorganisms on Al-Fe-oxides, Fe(III) is reduced to soluble Fe(II), and Al enrichment occurs, providing pathways for metal leaching and the beneficiation of bauxite ore. A salient feature is the elevated Li content in black coal seams and carbonaceous layers overlying the bauxite bodies [7]. However, since analytical data on the Li content in multicolor bauxite ores from the Parnassos–Ghiona Mountains are not available yet, the relationship between Li and Al_2O_3 (Figure 5) is still unclear.

Fe(II) may migrate, and pyrite is often located within the B3 horizon of the deposits, mostly towards the top of the bauxite ore bodies [42]. Mobilized iron, moving downward, can be re-precipitated as goethite, appearing with a deep red color (Figure 1d). Fine-grained framboidal pyrite is present as veins crosscutting previous phases, while veinlets of goethite crosscutting all previous minerals reflect the multistage formation of minerals at a wide range of Eh–pH conditions during the diagenetic and epigenetic stages [31,38].

5.2. Source and Economic and Genetic Significance of Lithium

The lightest lithophilic element, Li, is mainly concentrated in acidic igneous rocks and Al-sedimentary rocks. Lithium, as a cation of relatively small ionic radii, can easily substitute cations with sufficiently similar atomic radii, such as Al^{3+}, Mg^{2+}, and Fe^{2+}, in the minerals (micas and pyroxenes) of the pegmatites, as well as some sedimentary alumino-silicates [52]. During weathering, the released Li from the primary minerals, under oxidizing and acidic conditions, is incorporated in clay minerals and Fe-Al hydroxides, and/or is absorbed by organic matter, varying from 0.17 to 370 ppm Li in coal from the U.S., 50 to 1064 ppm Li in coal ash [53], 9 to 26 ppm in the Philippi (Eastern Macedonia, Greece) peat [54], 15 to 367 ppm Li in carbonaceous shales, and 16 to 367 ppm Li in coals, both overlying the Parnassos–Ghiona bauxite deposit [7]. The Li content in limited samples of bauxite ores from the Parnassos deposits ranged from <10 to 90 ppm, while in other karst-type bauxite deposits of the Balkan Peninsula, such as Montenegro in Serbia, it ranges from 257 to 486 ppm [8]. Relatively high values, 99–900 ppm Li in the bauxite ores and 53–354 ppm Li in overlying non-bauxite sediments, in the Cretaceous bauxite deposit of the Unterlaussa (Austria) [40] and Li super-enrichment in certain Permian karstic bauxite deposits in China, reaching up to 3390 ppm in the overlying carbonaceous clays [19] (Table 2), may indicate that the carbonaceous formation overlying the Li-bearing bauxite deposits are the major source of Li in the bauxite ore. Specifically, with respect to the Li-enriched clay rocks in China, it has been indicated that the main carrier mineral of Li is cookeite [$LiAl_4(Si_3Al)O.10(OH)_8$], which coexists with clay minerals (illite and pyrophyllite) [19]. Furthermore, the authors proposed that the cookeite originated from the reaction between clay minerals and Li-Mg-rich alkaline or pore–water extraction from thick bioclastic carbonate sediments, or from the direct replenishment of coastal underground brines [19]. Thus, given that the average Li concentration for world ocean water is 180 ppb Li [55], the much higher Li content in the associated coal seams compared to the bauxite ores, and the positive correlation between Li and B, both components of seawater, point to a Li enrichment through epigenetic processes (after their deposition) and the overlying coal seams as a major source for Li in of the Parnassos–Ghiona bauxite deposit. Therefore, the lower Li content in the Parnassos–Ghiona bauxite deposit compared to other karst-type deposits (Table 2) is likely related to the thin width of the overlying organic-rich rocks (less than 50 cm) and, in turn, the short time periods favorable for the development of small mires [7].

5.3. Implications of Critical Metals for the Exploration for Bauxites

The occurrence of abundant pyrite within the B3 third horizon of the Parnassos–Ghiona bauxite deposit, underlying faults, towards the top of the bauxite ore bodies, is commonly accompanied by the transformation of the red–brown bauxite to multicolor ore with intense changes in the mineralogy and geochemistry (Figures 1–5; Table 2). Although there are significant differences between the Cretaceous Parnassos–Ghiona and other karst-type bauxite deposits of Europe and China, in terms of the reserves, Li content, and thickness of the coal seams upper [7,19,40], the presence of organic matter as coal seams and/or carbonaceous shales may provide a carbon source for microorganisms, facilitating redox reactions, which is a common feature. The transportation of the Li from seawater (average 160 ppm) to sea plants and algae, which are components of Li in coal seams and carbonaceous sediments, is a potential pathway for the Li found in karst-type bauxite ores, both during bauxite precipitation and/or at a subsequent stage, due to degradation of the organic matter and Li in flowing rainwater. The mobilization of Fe(II) from pyrite, included either in coal [7] and/or in bauxite ore [5,6] during a subsequent stage, may be followed by re-oxidation of Fe(II) to Fe(III), appearing with a deep red color and yellow As-bearing minerals (Figure 1d). Thus, meteoric waters percolating along fractures and faults may result in the destruction of sulfides, creation of acidic solutions, and transformations in bauxite and the footwall-hanging wall limestone contact, providing evidence for the proximity to bauxite ore. Assuming that the major source of Li in karst-

type bauxites is the overlying organic-rich coals and carbonaceous sediments, during a post-deposition stage, despite the limited available analytical data, the relatively low Li content in the Parnassos–Ghiona deposits is consistent with the thin overlying coal seams and carbonaceous sediments. This points to a relatively low Li potential for these bauxite deposits.

5.4. Knowledge Gaps

The investigation of the Li distribution in the Parnassos–Ghiona, among the largest bauxite deposits of karst type, is based on limited literature data and a comparison with the other karst-type deposits. However, evaluating the Li potential and potential sources requires further primary research.

Although the preliminary data showed a positive trend between Li and Al_2O_3, this relationship has not been followed for the highest recorded Al_2O_3 contents. A large, more appropriate database for the explanation is needed. A characterization of Li-bearing minerals in the Parnassos–Ghiona deposit is also missing.

Furthermore, research is required to explain the much lower PGE content in karst-type bauxites compared to that of REE, occasionally reaching thousands of ppm. The elevated PGE content in Ni-laterites and the presence of PGE-bearing mineral compounds at the border of secondary Fe oxides support the PGEs' mobility during weathering. However, the much higher REE content in bauxites may reflect the higher mobilization of these metals under reducing and acidic conditions, and subsequently, re-deposition under favorable redox conditions, which may result in a significant REE content [28].

6. Conclusions

A comparison of the available geological, mineralogical, and geochemical data on the Parnassos–Ghiona karst-type bauxite deposit with those for other similar deposits allowed us to make preliminary conclusions and highlight the particular significance of the coal layers, carbonaceous layers, and overlying bauxite bodies to the source of Li and the exploration of karst-type bauxite deposits. The relatively high Li contents (hundreds ppm Li) in the bauxite ores and the greater Li contents in overlying non-bauxite sediments (mostly coal layers and carbonaceous clays) may indicate that these are major sources of Li in the bauxite ore.

The organic matter (derived from plants and algae growing in paleo-mires after regression of the sea) as coal and/or carbonaceous layers, overlying the karst-type bauxite deposits, as well as microorganisms, may be a driving force for redox reactions, potentially affecting the quality of the bauxite ore. Under reducing conditions, due to the degradation of organic matter, the Fe(III) reduces to Fe(II) in Al-Fe-oxides, providing pathways for metal leaching and the beneficiation of bauxite ore. Under a wide range of Eh–pH conditions during the post-deposition stages, fine-grained framboidal pyrite occurring in the B3 horizon towards the top of the bauxite deposit can be dissolved, producing acid solutions. The oxidation of the Fe(II) moving downward can be re-precipitated as goethite, appearing with a deep red color. The multistage formation of minerals in fragmented bauxite ore and the near boundary of the host limestone provides evidence for their proximity to bauxite deposits.

References

1. Bárdossy, G. *Karst Bauxites. Bauxite Deposits in Carbonate Rocks. Developments in Economic Geology*; Elsevier: Amsterdam, The Netherlands, 1982; Volume 14, 441p, ISBN 9780444597533.
2. USGS. *2018 Minerals Yearbook—Bauxite and Alumina [Advance Release]*; USGS: Reston, VA, USA, 2022; pp. 1–15.
3. Aronis, G. Geographical distribution, geological placing and aspects on the genesis of the Greek bauxite. *Bull. Geol. Soc. Greece* **1955**, *2*, 55–79. (In Greek)
4. Valeton, I.; Bierman, M.; Reche, R.; Rosenberg, F.F. Genesis of nickel laterites and bauxites in Greece during the Jurassic and the Cretaceous and their relation to ultrabasic rocks. *Ore Geol. Rev.* **1987**, *2*, 359–404. [CrossRef]
5. Laskou, M.; Economou-Eliopoulos, M. The role of microorganisms on the mineralogical and geochemical characteristics of the Parnassos-Ghiona bauxite deposits, Greece. *J. Geochem. Explor.* **2007**, *93*, 67–77. [CrossRef]
6. Laskou, M.; Economou-Eliopoulos, M. Bio-mineralization and potential biogeochemical processes in bauxite deposits: Genetic and ore quality significance. *Miner. Petrol.* **2013**, *407*, 171–186. [CrossRef]
7. Kalaitzidis, S.; Siavalas, G.; Skarpelis, N.; Araujo, C.V.; Christanis, C. Late Cretaceous coal overlying karstic bauxite deposits in the Parnassus-Ghiona Unit, Central Greece: Coal characteristics and depositional environment. *Int. J. Coal Geol.* **2010**, *81*, 211–226. [CrossRef]
8. Radusinović, S.; Papadopoulos, A. The Potential for REE and Associated Critical Metals in Karstic Bauxites and Bauxite Residue of Montenegro. *Minerals* **2021**, *11*, 975. [CrossRef]
9. Combes, P.-J. Regards sur la géologie des bauxites; aspects récents sur la genése de quelques gisements à substratum carbonate–A look at the geology of bauxite; recent data on the genesis of some deposits in carbonate rock. *Bull. Cent. Rech. Explor.-Prod. Elf-Aquitaine* **1984**, *8*, 251–274.
10. Šinkovec, B.; Sakac, K.; Durn, G. Pyritized bauxites from Minjera, Istria, Croatia. *Nat. Croat.* **1994**, *3*, 41–65.
11. Öztürk, H.; Hein, J.R.; Hanilçi, N. Genesis of the Doğankuzu and Mortaş bauxite deposits, Taurides, Turkey: Separation of Al, Fe, and Mn and implication for passive margin metallogeny. *Econ. Geol.* **2002**, *97*, 1063–1077. [CrossRef]
12. Gamaletsos, P.N.; Godelitsas, A.; Kasama, T.; Church, N.S.; Douvalis, A.P.; Göttlicher, J.; Steininger, R.; Boubnov, A.; Pontikes, Y.; Tzamos, E.; et al. Nano-mineralogy and geochemistry of high-grade diasporic karst-type bauxite from Parnassos-Ghiona mines, Greece. *Ore Geol. Rev.* **2017**, *84*, 228–244. [CrossRef]
13. Abedini, A.; Mehr, M.H.; Khosravi, M.; Calagari, A.A. Geochemical characteristics of the karst-type bauxites: An example from the Kanirash deposit, NW Iran. *Arab. J. Geosci.* **2019**, *12*, 475. [CrossRef]
14. Mondillo, N.; Di Nuzzo, M.; Kalaitzidis, S.; Boni, M.; Santoro, L.; Balassone, G. Petrographic and geochemical features of the B3 bauxite horizon (Cenomanian-Turonian) in the Parnassos-Ghiona area: A contribution towards the genesis of the Greek karst bauxites. *Ore Geol. Rev.* **2022**, *143*, 104759. [CrossRef]
15. Laskou, M.; Andreou, G. Rare earth element distribution and REE minerals from the Parnassos-Ghiona bauxite deposits, Greece. In *Mineral Exploration and Sustainable Development, Proceedings of the 7th Biennial SGA Meeting, Athens, Greece, 24–28 August 2003*; Eliopoulos, D., Baker, T., Barriga, F., Beaudoin, G., Benardos, A., Boni, M., Borg, G., Bouchot, V., Brown, A., Christidis, G., et al., Eds.; Millpress: Rotterdam, The Netherlands, 2003; pp. 89–92.
16. Deady, É.A.; Mouchos, E.; Goodenough, K.; Williamson, B.J.; Wall, F. A review of the potential for rare-earth element resources from European red muds: Examples from Seydişehir, Turkey and Parnassus-Giona, Greece. *Mineral. Mag.* **2016**, *80*, 43–61. [CrossRef]
17. Gamaletsos, P.N.; Godelitsas, A.; Filippidis, A.; Pontikes, Y. The rare earth elements potential of Greek bauxite active mines in the light of a sustainable REE demand. *J. Sustain. Metall.* **2019**, *5*, 20–47. [CrossRef]
18. Teichert, Z.; Bose, M.; Williams, L.B. Lithium isotope compositions of U.S. coals and source rocks: Potential tracer of hydrocarbons. *Chem. Geol.* **2020**, *549*, 119694. [CrossRef]
19. Ling, K.Y.; Wen, H.Z.; Zhang, Q.Z.; Luo, C.G.; Gu, H.N.; Du, S.J.; Yu, W.X. Super-enrichment of lithium and niobium in the upper Permian Heshan Formation in Pingguo, Guangxi, China. *Sci. China Earth Sci.* **2021**, *64*, 753–772. [CrossRef]
20. Zhang, J.Y.; Wang, Q.; Liu, X.F.; Zhou, G.F.; Xu, H.; Zhu, Y.G. Provenance and ore-forming process of Permian lithium-rich bauxite in central Yunnan, SW China. *Ore Geol. Rev.* **2022**, *145*, 104862. [CrossRef]
21. S&P Global Market Intelligence. Lithium M&A Involving Assets With Resources (2012–2019). 2021. Available online: https://www.spglobal.com/marketintelligence (accessed on 1 April 2023).
22. Kesler, S.E.; Gruber, P.W.; Medina, P.A.; Keoleian, G.A.; Everson, M.P.; Wallington, T.J. Global lithium resources: Relative importance of pegmatite, brine and other deposits. *Ore Geol. Rev.* **2012**, *48*, 55–69. [CrossRef]
23. Laskou, M. Concentrations of rare earths in Greek bauxites. *Acta Geol. Hung.* **1991**, *3*, 395–404.
24. Laskou, M. Geochemical and mineralogical characteristics of the bauxite deposits of western Greece. In *Mineral Exploration and Sustainable Development, Proceedings of the 7th Biennial SGA Meeting, Athens, Greece, 24–28 August 2003*; Eliopoulos, D., Baker, T., Barriga, F., Beaudoin, G., Benardos, A., Boni, M., Borg, G., Bouchot, V., Brown, A., Christidis, G., et al., Eds.; Millpress: Rotterdam, The Netherlands, 2003; pp. 93–96.
25. Pajović, M. Genesis and genetic types of karst bauxites. *Iran. J. Earth Sci.* **2009**, *1*, 44–56.
26. Pajović, M.; Radusinović, S. Stratigraphy of bauxites in Montenegro; Geological Survey of Montenegro, Podgorica. *Geol. Bull.* **2015**, *16*, 27–57.
27. Radusinović, S. Metallogeny of Jurassic Karstic Bauxites of Vojnik-Maganik and Prekornica Mining Areas, Montenegro. Ph.D. Thesis, University of Belgrade, Faculty of Mining and Geology, Belgrade, Serbia, 2017; pp. 1–349.

28. Economou-Eliopoulos, M.; Laskou, M.; Eliopoulos, D.G.; Megremi, I.; Kalatha, S.; Eliopoulos, G.D. Origin of Critical Metals in Fe-Ni Laterites from the Balkan Peninsula: Opportunities and Environmental Risk. *Minerals* **2021**, *11*, 1009. [CrossRef]

29. Pajović, M.; Radusinovićc, S. Mineral resources of Montenegro. Montenegro in the XXI century—In the Era of Competitiveness. The living environment and sustainable development. *Montenegrin Acad. Sci. Arts (Spec. Ed.)* **2010**, *73*, 237–282. (In Serbian, with English Abstract).

30. Gamaletsos, P. Mineralogy and Geochemistry of Bauxites from Parnassos-Ghiona Mines and the Impact on the Origin of the Deposits. Ph.D. Thesis, National and Kapodistrian University of Athens, Athens, Greece, 2014; p. 347.

31. Williams, R.J. Karst-Associated Bauxite Deposits of Parnassos-Ghiona, Central Greece: Ore Genesis and Structural Evolution. Ph.D. Thesis, University of Brighton, Brighton, UK, 2014.

32. Laskou, M.; Economou, M. Palladium, Pt, Rh and Au Contents in Some Bauxite Occurrences of Greece. In Proceedings of the Balkan-Carpathian Congress, Sofia, Bulgaria, 11–13 December 1989; pp. 1367–1371.

33. Laskou, M. Pyrite-rich bauxites from the Parnassos-Ghiona zone, Greece. In *Mineral Deposit Research: Meeting the Global Challenge*; Mao, J., Bierlein, F.P., Eds.; Springer: Berlin/Heidelberg, Germany, 2005; pp. 1007–1010.

34. Lu, F.H.; Xiao, T.F.; Lin, J.; Li, A.J.; Long, Q.; Huang, F.; Xiao, L.H.; Li, X.; Wang, J.W.; Xiao, Q.X.; et al. Recovery of gallium from Bayer red mud through acidic-leaching-ion exchange process under normal atmospheric pressure. *Hydrometallurgy* **2018**, *175*, 124–132. [CrossRef]

35. Williams-Jones, A.E.; Vasyukova, O.V. The Economic Geology of Scandium, the Runt of the Rare Earth Element Litter. *Econ. Geol.* **2018**, *113*, 973–988. [CrossRef]

36. Dragovic, D. The red and white karstic bauxites of Montenegro (Yugoslavia). *Travaux* **1989**, *19*, 249–257.

37. Tang, B.; Fu, Y.; Yan, S.; Chen, P.-W.; Cao, C.; Guo, C.; Wu, P.; Long, Z.; Long, K.-S.; Wang, T.-S.; et al. The source, host minerals, and enrichment mechanism of lithium in the Xinmin bauxite deposit, northern Guizhou, China: Constraints from lithium isotopes. *Ore Geol. Rev.* **2022**, *141*, 104653. [CrossRef]

38. Putzolu, F.; Papa, A.P.; Mondillo, N.; Boni, M.; Balassone, G.; Mormone, A. Geochemical Characterization of Bauxite Deposits from the Abruzzi Mining District (Italy). *Minerals* **2018**, *8*, 298. [CrossRef]

39. Mongelli, G.; Buccione, R.; Gueguen, E.; Langone, A.; Sinisi, R. Geochemistry of the apulian allochthonous karst bauxite, Southern Italy: Distribution of critical elements and constraints on Late Cretaceous Peri-Tethyan palaeogeography. *Ore Geol. Rev.* **2016**, *77*, 246–259. [CrossRef]

40. Hampl, F.J.; Melcher, F. The formation of the Unterlaussa karst bauxite (Austria)—A re-evaluation of the established model. *J. Geochem. Explor.* **2023**, *245*, 107141. [CrossRef]

41. Liu, X.; Zhong, Y.; Zhu, S.; Zhang, S.; Cao, J. Study on the properties of bauxite modified by acid leaching and calcination for improving fluorine removal. *Asia-Pac. J. Chem. Eng.* **2023**, *18*, e2839. [CrossRef]

42. Economou-eliopoulos, M.; Kontou, M.; Mrgremi, I. Biogeochemical Redox Processes Controlling the Element Cycling: Insights from Karst-Type Bauxite, Greece. *Minerals* **2022**, *12*, 446. [CrossRef]

43. Ochsenkühn-Petropulu, M.; Lyberopulu, T.; Parissakis, G. Direct determination of lanthanides, yttrium and scandium in bauxites and red mud from alumina production. *Anal. Chim. Acta* **1994**, *296*, 305–313. [CrossRef]

44. Wagh, A.S.; Pinnock, W.R. Occurrence of scandium and rare earth elements in Jamaican bauxite waste. *Econ. Geol.* **1987**, *82*, 757–761. [CrossRef]

45. Boni, M.; Rollinson, G.; Mondillo, N.; Balassone, G.; Santoro, L. Quantitative mineralogical characterization of karst bauxite deposits in the Southern Apennines, Italy. *Econ. Geol.* **2013**, *108*, 813–833. [CrossRef]

46. Borra, C.R.; Pontikes, Y.; Binnemans, K.; Van Gerven, T. Leaching of rare earths from bauxite residue (red mud). *Miner. Eng.* **2015**, *76*, 20–27. [CrossRef]

47. Roosen, J.; Van Roosendael, S.; Borra, C.R.; Van Gerven, T.; Mullens, S.; Binnemans, K. Recovery of scandium from leachates of Greek bauxite residue by adsorption on functionalized chitosan-silica hybrid materials. *Green Chem.* **2016**, *18*, 2005–2013. [CrossRef]

48. Russell, M.J.; Hall, A.J.; Boyce, A.J.; Fallick, A.E. 100th Anniversary special paper: On hydrothermal convection systems and the emergence of life. *Econ. Geol.* **2005**, *100*, 419–438. [CrossRef]

49. Baskar, S.; Baskar, R.; Kaushik, A. Role of microorganisms in weathering of the Konkan-Goa laterite formation. *Curr. Sci.* **2003**, *85*, 1129–1134.

50. Southam, G.; Saunders, J. The geomicrobiology of ore deposits. *Econ. Geol.* **2005**, *100*, 1067–1084. [CrossRef]

51. Ehrlich, H.; Witkowski, A. Biomineralization in Diatoms: The Organic Templates. In *Evolution of Lightweight Structures. Biologically-Inspired Systems*; Hamm, C., Ed.; Springer: Dordrecht, The Netherlands, 2015; Volume 6.

52. Kabata-Pendias, A. *Trace Elements in Soils and Plants*; CRC Press, Inc.: Boca Raton, FL, USA, 2000; p. 550.

53. Finkelman, R.B. Trace elements in coal. Environmental and health significance. *Biol. Trace Element. Res.* **1999**, *67*, 197–204. [CrossRef] [PubMed]

54. Christanis, K.; Georgakopoulos, A.; Fernandez-Turiel, J.L.; Bouzinos, A. Geological factors influencing the concentration of trace elements in the Philippi peatland, eastern Macedonia, Greece. *Int. J. Coal Geol.* **1998**, *36*, 295–313. [CrossRef]

55. Reimann, C.; de Caritat, P. *Chemical Elements in the Environment*; Springer: Berlin/Heidelberg, Germany, 1998; p. 398.